Life Cycle Analysis of a PEM Fuel Cell System for Long-Haul Heavy-Duty Trucks

2024-24-0020 Published 18 Sep 2024

Life Cycle Analysis of a PEM Fuel Cell System for Long-Haul Heavy-Duty Trucks

Gaia Gentilucci, Antonella Accardo, and Ezio Spessa Politecnico di Torino

Citation: Gentilucci, G., Accardo, A., and Spessa, E., "Life Cycle Analysis of a PEM Fuel Cell System for Long-Haul Heavy-Duty Trucks," SAE Technical Paper 2024-24-0020, 2024, doi:10.4271/2024-24-0020.

Received: 05 May 2024 Revised: 30 Jun 2024 Accepted: 08 Jul 2024

Abstract

The European Union plans to reach net-zero greenhouse gas (GHG) emissions in 2050. In 2020, the transport sector significantly contributed to global energy-related GHG emissions, with heavy-duty vehicles (HDVs) responsible for a substantial portion of road transport emissions in the EU and a notable percentage of the EU's total GHG emissions. Zero-emission vehicles (ZEVs), including fuel cell (FC) vehicles, are crucial for decarbonizing the transport sector to achieve climate neutrality. This paper aims at quantifying the environmental impacts of a 200kW proton exchange membrane FC system for long-haul HDVs with a 40-ton mass and 750 km driving range. The life cycle assessment (LCA) methodology was applied, and a life cycle model of the FC system was developed with a cradle-to-grave boundary. To ensure reproducibility and scalability, results are reported on a kW basis. A sensitivity analysis was performed on key parameters, including hydrogen production route, FC system production location, fuel consumption, FC system size, FC system replacement, and FC material composition. At the cradle-to-gate boundary, GHG emissions of the FC system ranged from 30.5 to 51.4 kg CO_2eq/kW. The catalyst was the most impactful component due to the presence of platinum, followed by the balance of plant. In the cradle-to-grave boundary, raw material extraction and production phases were negligible, while the use phase was the main driver of the overall impact of the FC system. Certain equivalences were observed when considering other impact categories.

1. Introduction

The European Union is aiming to achieve climate neutrality by 2050 [1]. In 2020, the transport sector accounted for 27% of global energy-related greenhouse gas (GHG) emissions [2]. Particularly heavy-duty vehicles (HDVs) are responsible for more than 25% of GHG emissions from road transport in the EU, and for over 6% of total EU GHG emissions [1]. On February 9th, 2024, the Council and the European Parliament reached a provisional agreement on CO_2 emission standards for HDVs [3,4]. The goal is to further decrease CO_2 emissions in the road transport sector setting new targets for 2030 (45%), 2035 (65%), and 2040 (90%) for HDVs over 7.5 tons and to promote the use of zero-emission vehicles (ZEVs) in the EU-wide HDV fleet [3]. According to [5], zero-emission heavy-duty vehicle' are those HDVs without an internal combustion engine or with an internal combustion engine that emits not more than 3 g CO_2/(tkm) or 1 g CO_2/(pkm) such as Fuel Cell Electric Vehicles (FCEVs). Also, the Commission will investigate by 2027 the potential for creating a standardized methodology to evaluate and report the complete life cycle greenhouse gas (GHG) emissions of new HDVs [3]. The Life Cycle Assessment (LCA) methodology can be used to assess the total GHG emissions produced across a product's entire life cycle. An LCA study can reveal the advantages and disadvantages of replacing one powertrain technology with another [6]. Many studies on the LCA of Fuel Cell (FC) systems or FC vehicles have been carried out.

At vehicle level, [7] proposed the LCA of Toyota Mirai paying attention to the detailed vehicle component breakdown focusing on the Chinese context. Bekel and Pauliuk [8] compared the LCA of a mid-size FCEV and a Battery Electric Vehicle (BEV) (i.e., VW e-Golf and Toyota Mirai) focusing on the fuel supply infrastructure. Drawer et al. [9] performed an LCA study aimed at assessing the environmental impacts of a retrofitted FC truck from a used diesel truck. Evangelisti et al. [10] compared three different passenger cars, i.e., BEV, FCEV, and Internal Combustion Engine Vehicle (ICEV), by means of LCA and paying attention to the manufacturing phase. Miotti et al. [11] performed a similar comparative assessment for class C vehicles, integrating with economic assessment and providing forecasts for 2030. Simons and Azimov [12] compared the LCA of BEV, FCEV and ICEV powertrains for heavy-duty applications. Lastly, [13] carried out a comparative LCA focused on the difference between

Proton Exchange Membrane Fuel Cells (PEMFCs) and solid oxide fuel cells for passenger car applications. For LCAs at vehicle level, the use phase is a critical aspect. Fuel consumption values vary widely in the literature. Fuel consumption data differ significantly among various literature sources and data are scarce for HDVs. In fact, according to [6], fuel consumption ranges between 0.58 and 1.15 kg H_2/100 km, but all refer to passenger cars. Moreover, an important aspect of the life cycle of a FCEV is the assumed hydrogen production route. Simons et al. [14] stated that the hydrogen use and, therefore, the efficiency of the fuel cell system and the method of hydrogen production, is the decisive factor in the environmental performance.

At FC system level, [14] performed the LCA of PEMFCs for passenger cars. Here, it was found that one of the main drivers of the GHG emissions of the PEMFC is the use of platinum as catalyst material and the reduction of catalyst loading can significantly benefit the carbon footprint [14]. In [6], the authors investigated the effect of durability and performance losses of fuel cells on the life-cycle environmental impact of the vehicle. The FC durability resulted as a fundamental parameter for the life cycle impacts of FCEVs, being the performance losses significant drivers of the fuel consumption and, thus, of the GHG emissions during the use phase [6]. Lastly, [15] assessed the environmental benefits of a novel recycling process for recovery the platinum catalyst in the Membrane Electrode Assembly (MEA), one of the key components of PEMFCs. The results show that the impacts of the MEA life cycle can be significantly reduced if platinum is recovered in the end-of-life (EoL) of the product [15].

In this context, the present study aims at contributing to the development of a LCA methodology to be applied on FC systems suitable for heavy-duty FCEVs and long-haul delivery operations. This research is part of the activities of the Horizon Europe "Eco-operated, Modular, highly efficient, and flexible multi-POWERtrain for long-haul heavy-duty vehicles" (EMPOWER) project.

The novelty of this research lies in the application of the LCA methodology specifically to HDVs utilizing a FC as their powertrain. This represents a significant advancement, as the majority of existing studies have focused on FC mounted on passenger cars, where the parameters considered, such as hydrogen consumption and operational conditions, differ substantially. Consequently, this study provides a unique perspective by addressing the environmental impacts associated with FC-powered HDVs. The primary objective of this study is to comprehensively evaluate the environmental impacts of FC systems mounted in a HDV by varying several critical parameters. These parameters include the FC material composition, the rate of fuel consumption, the size of the system, the frequency of FC replacements, and the H_2 production routes. By systematically analyzing these variables, the study aims to identify the key factors influencing the environmental performance of FC, thereby contributing valuable insights into the optimization of these systems for reduced environmental impact

2. Materials and Methods

2.1. Goal and Scope Definition

The first stage of an LCA study is the goal and scope definition. The goal of this study is to perform the LCA of a PEMFC system suitable for a long-haul heavy-duty truck characterized by a mass of 40 tons, a driving range of 750 km and a lifetime of 700,000 km. The LCA performed in the present study follows the ISO standards 14040 and 14044 [16,17] and the FC-Hy guide [18], a specific guidance for performing LCAs on fuel cells and hydrogen technologies. Two system boundaries have been considered in this study (Figure 1). To compare different FC systems in terms of material composition, a cradle-to-gate boundary has been adopted. Then, to assess the complete LCA of the FC system under study, the system boundary has been enlarged to the cradle-to-grave scope. The cradle-to-gate boundary comprises raw material acquisition and preprocessing, and manufacturing of FC components while the cradle-to-grave boundary comprises raw material acquisition and preprocessing, manufacturing of FC components, transport of materials and FC components, the Well-to-Tank (WTT) emissions during use, and EoL. For the functional unit, it is a very variable assumption in the literature. In [10], the functional unit is 1 km driven by one vehicle. Instead, in [19] the functional unit is 1 ton of transported goods over a distance of 1 km (tkm). To ensure comparison across different FC systems, 1 kW of the maximum power of the FC system has been assumed as the functional unit in the cradle-to-gate boundary in compliance with the FC-Hy guide [18]. Instead, one heavy duty truck is assumed as the functional unit in the cradle-to-grave boundary. In addition, because the vehicle under study is still under design, a scenario analysis has been carried out on certain key parameters of the FC system to evaluate how the

FIGURE 1 System boundary definition

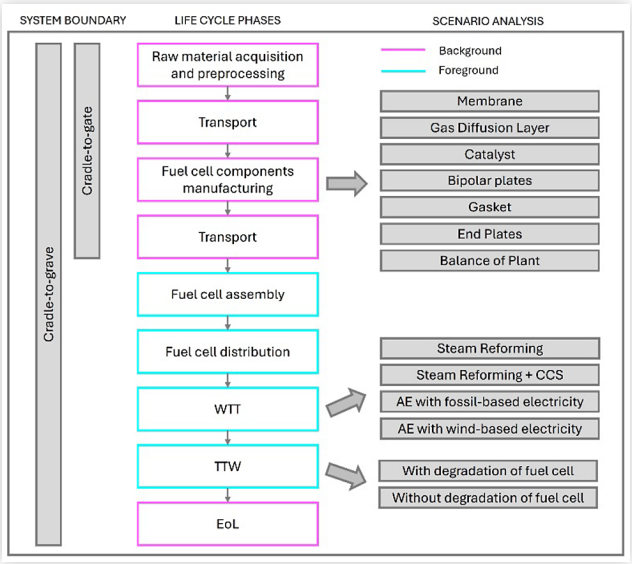

environmental impacts vary as some important parameters change. For the LCA model, SimaPro v.9.4.0.3 has been used as the LCA software [20] and Ecoinvent 3.8 at the point of substitution (APOS) database has been used as the background database [21]. The assessment has been conducted on a broad range of environmental impacts, adopting the EF3.0 life cycle impact assessment method as suggested by the European Commission's Product Environmental Footprint (PEF) method [22]. The EF3.0 method is an essential component of the PEF initiative, which aims to standardize the assessment process, to facilitate more consistent and comparable evaluations of environmental performance, thereby to support regulatory policies, to enhance decision-making, and to promote sustainability at both regional and global levels.

2.2. Data Analysis

The second stage of an LCA study is the life cycle inventory (LCI) creation that involves data collection and calculation procedures to quantify relevant inputs and outputs of the FC product system under study [23]. During this phase, different scenarios have been set up to deeply understand the main hotspots of common FC systems and to take into account potential variations, in terms of material breakdown, well-to-thank emissions, and performance characteristics. To accomplish this goal, first, a literature review focused on the LCA of FC systems has been carried out. Several features have been considered to filter the search, namely, the topic (only publications focused on PEMFCs have been considered), the study type (only LCA studies have been considered), the presence of transparent and replicable LCIs, and the publication year (only publications published after 2015 have been considered). Then, the scenario analysis has been carried out on the cradle-to-gate boundary, varying the material breakdown of the FC system to highlight the most impactful materials and the production site to highlight the relevance of the country electricity mix. Lastly, the scenario analysis has been carried out on the well-to-tank emissions and main performance characteristics of the FC system with respect to its intended application, i.e., varying the fuel consumption, the hydrogen production route, the system size, and durability. As a summary, five scenarios have been set up, namely Scenario A, Scenario B, Scenario C, Optimistic, and Pessimistic (Tables 1-2). Scenarios A, B, and C differ in terms of material breakdown and hydrogen production route, while optimistic and pessimistic scenarios have been set up to respectively combining the best and worst parameters of scenarios A, B, and C in terms of GHG emissions.

2.2.1. Scenario Set-Up Table 1 reports the scenario parameters related to the material breakdown of the FC system for the five scenarios under study. A fuel cell stack is comprised of several membrane electrode assembly (MEA) and bipolar plates (BPP) placed successively

TABLE 1 Fuel cell material compositions

Parameter	Scenario A	Scenario B	Scenario C	Optimistic	Pessimistic
Production site	GLO	GLO	GLO	EU	CN
Membrane	Tetrafluoroethylene (TFE): 96% Sulfuric acid: 4% [11]	Tetrafluoroethylene (TFE): 57,4% Sulfuric acid: 42,6% [14]	Tetrafluoroethylene (TFE): 52% Sulfuric acid: 39% Titanium dioxide: 9% [14]	Tetrafluoroethylene (TFE): 57,4% Sulfuric acid: 42,6% [14]	Tetrafluoroethylene (TFE): 96% Sulfuric acid: 4% [11]
GDL	Carbon fiber reinforced plastic: 74% TFE:11% Carbon black:14% Solvent:1% [11]	Carbon fiber reinforced plastic: 60% TFE:12% Carbon black:22% Solvent:7% [11]	Carbon cloth: 81% TFE: 14% Carbon black: 5%[14]	Carbon fiber reinforced plastic: 60% TFE:12% Carbon black:22% Solvent:7% [11]	Carbon cloth: 81% TFE: 14% Carbon black: 5%[14]
Catalyst	Pt loading:0,4 mg/cm^2 Platinum:10% Carbon black: 3% TFE: 0,4% Solvent:86,6% [11]	Pt loading:0,2 mg/cm^2 Platinum: 5,3% Carbon black: 1.6% TFE: 0,2% Solvent:92.9% [11]	Pt loading:0,2 mg/cm^2 Platinum (5% recycled): 5,3% Carbon black: 1.6% TFE: 0,2% Solvent:92.9%	Pt loading:0,2 mg/cm2 Platinum (5% recycled): 5,3% Carbon black: 1.6% TFE: 0,2% Solvent:92.9%	Pt loading:0,4 mg/cm^2 Platinum:10% Carbon black: 3% TFE: 0,4% Solvent:86,6% [11]
Bipolar plates	Graphite: 69% phenolic resin: 29% [11]	Chromium steel: 85% Titanium dioxide: 7% Graphite: 7% Phenolic resin: 1% [11]	Chromium steel: 96% Titanium dioxide: 2% Graphite: 2%[14]	Graphite: 69% phenolic resin: 29% [11]	Chromium steel: 85% Titanium dioxide: 7% Graphite: 7% Phenolic resin: 1% [11]
Gasket	Polysulfide [11]	Synthetic rubber [10]	N	N	Synthetic rubber [10]
End of plates, collectors	Glass fiber: 50% Epoxy resin: 50% [11]	Aluminum [14]	Aluminum [14]	Glass fiber: 50% Epoxy resin: 50% [11]	Aluminum [14]

TABLE 2 Scenario parameters related to the use phase emissions and performance characteristics of the FC system with respect to its intended application

Parameter	Scenario A	Scenario B	Scenario C	Optimistic	Pessimistic
Fuel consumption (kg H_2/km)	0.0845	0.0845	0.0845	0.0845	0.0963
System size (kW)	200	200	200	200	400
FC replacement	N	N	N	N	Y
H2 production	SMR	SMR with CCS	AE with fossil-based electricity	AE with wind-based electricity mix	SMR

between current collectors and packed with two end-plates (EP), nuts and bolts [24]. A MEA is a stack cell comprising two gas diffusion layers (GDL), two electrodes (an anode and a cathode) and an ion conducting membrane that is occasionally supported by a polymeric gasket [24]. The number of MEA in a fuel cell influences the power of the system. Table 1 reports the scenario parameters related to the material breakdown of the FC system for the five scenarios under study. In this study, a variation of material composition of certain FC components (i.e., membrane, GDL, catalyst, BPP, EP and gasket) has been performed. In addition, different geographical boundaries have been considered to evaluate how much the production location affects the environmental impacts. While scenarios A, B, and C share a global average (GLO) scope, Europe (EU) has been adopted for the optimistic scenario, and China (CN) has been adopted for the pessimistic scenario as the FC system production locations.

For the membrane, it separates the reduction and oxidation reactions, allowing the protons to pass through to complete the overall reaction and the electrons, created on the anode side, to flow through an external circuit, creating current [10]. Almost all commercially available membranes for PEMFCs are based on perfluorosulfonic acid (PFSA) [25]. The most commonly used PFSA for PEMFCs is Nafion (DuPont). Nafion is prepared via the copolymerization of variable amounts of unsaturated perfluoroalkyl sulfonyl fluoride (PSF) with tetrafluoroethylene (TFE) [25]. For modelling the production process of PSF, the Ecoinvent dataset representative of sulfuric acid production has been used as proxy. Scenarios A and B are based on different sources [11,14] and differ only in the percentage composition of materials (TFE and sulfuric acid) while in scenario C a percentage of titanium dioxide has been added with the function of hydrophilic additives (Table 1). In fact in the case of TiO_2, adding at a level of 10 wt.% would raise the density of the membrane to around 2.17 g/cm^3 [14].

GDLs play multiple roles, including electronic connection between the channel-land structured bipolar plates and the catalyst layer (CL), passage for reactant, transport and heat/water removal, mechanical support to the membrane and CLs and protection of the CL from corrosion or erosion caused by flows or other factors [26]. The most common materials for GDL are woven or non-woven carbon fibers which provides high electrical conductivity and a porosity greater than 70%, whilst simultaneously having high stability and resistance to corrosion [14]. In scenarios A and B, GDL is made up of non-woven carbon substrate macroporous layer with a microporous layer of TFE and carbon black based on [11]. In scenario C, a carbon cloth material coated with TFE and carbon black has been assumed for the GDL in compliance with [14]. The woven carbon cloth, unlike carbon paper, does not need a resin binder [14]. The carbon cloth is made from carbon fiber [10].

The role of the catalyst is to facilitate the electrochemical reactions and provide pathways for both reactant transport and electron/proton conduction [26]. The catalyst is commonly prepared in the form of an ink [10]. The most widely employed catalyst in PEM fuel cells is platinum, which is implemented in both anode and cathode. A wet catalyst solution composed of Pt/C, carbon black as a porous conductive material, TFE and solvent has been assumed in the present study in compliance with [11]. The scenarios in Table 1 differ in terms of platinum loading. Moreover, in scenario C and in the optimistic scenario, the use of 95 % primary platinum and 5 % secondary (i.e., recycled) platinum has been assumed.

The bipolar plate have several functions within the fuel cell: distribute the fuel and oxidant within the cell; facilitate water and heat management; separate different cells in the stack; and carry electrical current from the cell [27]. For automotive applications it is important that the bipolar plates are lightweight and able to be easily manufactured from inexpensive materials. They can be made out of non-porous graphite, specific metals and alloys or polymer composite materials [14]. Based on [11], the bipolar plates of scenario A have been assumed to be composed of graphite and phenolic resin, while the bipolar plates of scenario B have been assumed to be composed of chromium steel, titanium, graphite and phenolic resin. Scenario C is the same as scenario B but without phenolic resin [14].

The gaskets seal the MEA to the bipolar plate [10]. It has been assumed that the gaskets are composed of polysulfide in scenario A as in [11] or synthetic rubber in scenario B as in [10]. Scenario C, instead, has no gasket in compliance with [14].

End plates are the components that, together with tie rods, clamp the fuel cells together in the form of a stack [28]. The end plates components have been assumed to be composed of aluminum in scenarios B and C, in compliance with [14], while they have been assumed to be composed of glass fiber and epoxy resin in scenario A, in compliance with [11].

The Balance of Plant (BoP) consists of essential and ancillary components needed to complete the fuel cell system. It is divided into four main management systems: air, water, thermic and fuel. In this way, each system is

responsible for the management of different aspects related to the operation of the overall fuel cell system. BOP and ancillary components represent a significant weight/volume as well as cost contribution to the overall PEMFC system cost. According to [29], the BOP may occupy up to 60% of the total system volume. In this work, the BoP is modelled following the approach outlined in [11]. The BOP comprises the following components:

- the air management system with compression expansion motor (CEM), air filter, air ducting;
- the water management system with humidifier, Nafion tubes, air preecoler, demister;
- the heat management system with high temperature loop (HTL) and low temperature loop (LTL);
- the fuel management system with ejectors, pipes, valves, inline filter, pressure switch;
- the control system with hydrogen sensor, other sensors, control electronics;
- other components including wiring, belly pan, mounting frames and fasteners.

The hydrogen tank is excluded from the system boundary of this study.

Table 2 reports the scenario parameters related to the well-to-tank emissions and performance characteristics of the FC system with respect to its intended application for the five scenarios under study. The intended application is a novel FCEV suitable for long-haul operation conditions with a maximum unrefueled range of 750 km, providing a payload capacity ≥ 90% of the payload of the comparable diesel-powered truck and to be developed as a prototype in the Europe-funded EMPOWER project. In fact, among the objectives of EMPOWER, there is the development of a modular and flexible FCEV with a Combined Gross Vehicle Weight (C-GVW) [1] of at least 40 tons, ready to enter the market in 2029 at TRL 8. The prototype will be developed starting from an existing Internal Combustion Engine (ICE) 6x2 rigid truck platform of VECTO group 9, modifying certain areas (e.g., the engine bay area, low-voltage architecture, frame layout, rear suspension), and introducing new developed systems (e.g., climatization system of the cabin, e-axle, battery system, fuel cell system, electric brakes, thermal management system). The FCEV under study is equipped with a battery system, comprised of two lithium-ion battery packs and a central battery management system (BMS), and a 200-kW fuel cell system. Batteries are required for fast provision of electric power in transient driving conditions when the power increase by the fuel cell system is not fast enough. They also serve as a buffer of energy balancing the power requirements. In downhill conditions the e-axle can serve as an electric generator, charging the batteries. Hence the overall net consumption of energy will be partially recuperated and stored in the batteries. This configuration has been chosen to ensure comfortable driving characteristics and vehicle speeds comparable to ICE-trucks currently used on the trans-alpine corridor. A dual e-drives e-axle layout comprised of two permanent magnet synchronous electric motors and an IGBT inverter is considered to achieve the targeted performance. Hydrogen will be stored in five tanks, three of them mounted in a dedicated structure behind the cabin, and two of them directly on the chassis (one on each side).

The fuel consumption of the present study has been estimated through a simulation model of the FCEV, considering a VECTO long-haul driving cycle, resulting in 0.0845 kg H_2/km, in scenarios A, B, C, and optimistic [30]. However, according to [31], the amount of required hydrogen can be heavily influenced by PEMFC degradation, so that a hydrogen vehicle with a degraded fuel cell consumes 14.3% more fuel than a fresh fuel cell hydrogen vehicle. Therefore, a hydrogen consumption of 0.0963 kg H_2/km has been explored in the pessimistic scenario to investigate the reduction of performance in the event of PEMFC degradation.

For what concerns the system size, the maximum power of the studied FC system is 200 kW, but an additional scenario with a 400-kW FC system has been investigated and evaluated in the pessimistic scenario. In fact, while the 200-kW system configuration, allows for enough efficiency and power to cover the trans-alpine mission requirements of the case-study vehicle, the 400-kW system configuration would allow for outstanding efficiency and power levels at the expense of increased weight and cost.

Lastly, four hydrogen production routes have been investigated: steam methane reforming (SMR), steam methane reforming with carbon capture and storage (SMR-CCS), water alkaline electrolysis (AE) with fossil-based electricity and with wind-based electricity. The former is based on the current EU electricity mix while the latter is based on a potential green electricity mix composed of the mix of Netherlands (3.9%) and offshore wind electricity (96.1%). SMR has been assumed as production route in the pessimistic scenario because it is the current most used production method in Europe while AE with wind-based electricity has been assumed as production route in the optimistic scenario as representative of future promising technology in terms of decarbonization potential.

3. Results

3.1. Climate Change Results at the Cradle-to-Gate Boundary

Figure 2 shows the cradle-to-gate climate change results, i.e., Global Warming Potential (GWP) or GHG emissions, per functional unit. All the scenarios considered in this study are shown. Each bar highlights the contributions of the fuel cell components in different colors, i.e., end plates in red, bipolar plates in indigo, catalyst in dark blue, gasket

[1] Combined Gross Vehicle Weight (C-GVW) comprises both vehicle and trailer weights

FIGURE 2 Climate change results for the cradle-to-gate boundary per kW peak power

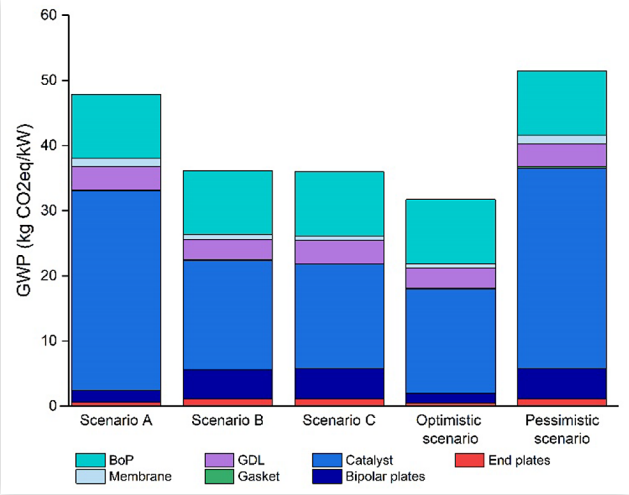

in green, GDL in purple, membrane in light blue, and BOP in turquoise.

For scenario A, the GWP is 47.9 kg CO_2eq/kW. The platinum contained in the catalyst is the main contributor to this impact, accounting for about 64% of the overall FC system impact. This is because platinum production, including mining, processing, and refining, involves significant energy consumption and GHG emissions. The BOP is the second contributor because of the significant GWP impact of the carbon fiber reinforced plastic contained in the belly pan component and the copper contained in the cable conductor. In fact, the production of precursor materials used in carbon fiber production, such as polyacrylonitrile (PAN), requires significant amounts of energy and leads to the release of GHGs. Furthermore, the process of creating carbon fiber reinforced plastic involves the use of resins, usually derived from petrochemicals, which emit GHGs and release volatile organic compounds (VOCs) during curing. As with platinum, copper production typically involves energy-intensive processes such as mining, extraction, smelting, and refining. These processes often require significant amounts of energy, which are typically derived from fossil fuels. The GDL is the third contributor due to the presence of carbon fiber reinforced plastic and tetrafluoroethylene (TFE). TFE is used as a precursor in the production of polytetrafluoroethylene (PTFE), commonly known as Teflon. The production of TFE and PTFE involves the use of perfluorocarbons (PFCs), which are potent GHGs with high GWPs.

For scenario B, the GWP is 36.2 kg CO_2eq/kW. This is mainly driven by the presence of platinum in the catalyst, even though the impact of catalyst is reduced from 64% to 46% with respect to the overall FC system because platinum is present in smaller amounts (0.2 mg/cm^2 in scenario B vs 0.4 mg/cm^2 in scenario A). In scenario B, the BOP represents the second largest contributor in terms of climate change accounting for 27 %. Lastly, the BPP plays an important role. In fact, it contributes by 12% to the total impact of the FC system (in scenario A it contributes only 4%) due to the presence of chromium steel. The extraction and processing of raw materials for chromium steel production significantly contributes to its environmental footprint in terms of climate change.

In scenario C, climate change accounts for 35.9 kg CO_2eq/kW. The main contributor to this impact is the platinum contained in the catalyst. In fact, the catalyst contributes 45%. In this scenario, the platinum quantity remains same as in scenario B, but 5% of recycled platinum has been taken into account. However, the use of recycled platinum is revealed to not significantly reduce climate change. Also, in this scenario, BOP and GDL affect the total impact by 27% and 13%, respectively.

In the optimistic scenario, the GWP is 30.5 kg CO_2eq/kW. This is the lowest GWP among the investigated scenarios. The main reason is the lower amount of platinum in the catalyst. Also, the assumed production site strongly influences the GWP; in fact, it is assumed that raw materials and FC component productions take place in Europe, which has made significant strides in transitioning to cleaner energy sources, including renewables and natural gas, which can lead to lower emissions associated with manufacturing processes.

In the pessimistic scenario, the GWP is 51.4 kg CO_2eq/kW. In this case the assumed production site is China. Indeed, China's energy mix is still heavily reliant on coal, which is a significant a source of GHG emissions. The use of coal in energy production results in higher carbon dioxide (CO_2) emissions compared to cleaner energy sources such as natural gas or renewable energy.

In terms of cradle-to-gate GWP, the results of the present study resulted to be consistent with values reported in the literature (Table 3). Specifically, the GWP values range from a minimum of 29 kgCO_2eq/kW to a maximum of 57.9 kgCO_2eq/kW, and the findings of this study fall within this range. The variability in GWP values can be attributed to factors such as the type and quantity of materials used in fuel cell components, the manufacturing location, and the associated electricity mix.

3.2. Climate Change Results at the Cradle-to-Grave Boundary

Figure 3 shows the cradle-to-grave climate change results. All the scenarios considered in this study are shown. Each bar highlights the contribution of the cradle-to-gate emissions in red, use phase emissions in indigo, and EoL emissions in dark blue. For scenario A, the GWP is 9.1E5 kg CO_2

TABLE 3 GWP results comparison at cradle-to-gate boundary

GWP results kgCO_2eq/kW	Present work	Miotti et al. (2015)	Evangelisti et al. (2017)	Benitez et al. (2020)	Usai et al. (2021)
Cradle-to-gate	30.5-51.4	29[11]	57.9[10]	31.7[32]	37.3[33]

FIGURE 3 Climate change results for the cradle-to-grave boundary

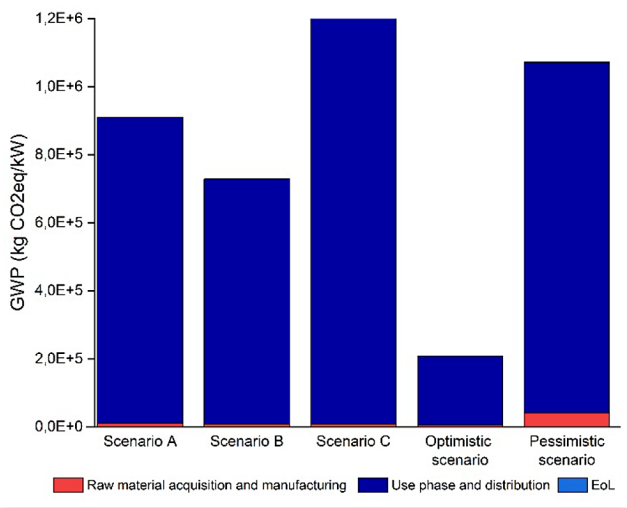

eq. The largest contribution is the use phase (99%), in which SMR has been assumed as hydrogen production route. In scenario B, the GWP is 7.3E5 kg CO_2 eq. The largest contribution is the use phase (99%), in which SMR with CCS has been assumed as hydrogen production route. From scenario A to scenario B, the GWP has been reduced by 20%, and this is mainly due to the assumed hydrogen production route. In scenario B, in fact, the CO_2 produced during the reforming process is partially captured rather than being released into the atmosphere. By capturing and storing CO_2, SMR with CCS prevents it from contributing to the greenhouse effect and accumulating in the atmosphere. In scenario C, the GWP is 1.3E6 kg CO_2 eq. This impact is mainly driven by the assumed hydrogen production route, i.e., AE with fossil-based electricity. Contrarily, in the optimistic scenario, the hydrogen production route is AE based on wind electricity. The use of green energy in this case strongly influences the GWP, which is 2.1E5 kg CO_2eq, accounting for a reduction rate of 80% with respect to scenario C. Under the pessimistic scenario, the GWP is 1.1E6 kg CO_2eq. SMR has been assumed as production route in this scenario, which strongly affects the results. As in the other scenarios, the use phase resulted in the most impactful phase. Nevertheless, against the previous scenarios, the contribution from raw material acquisition, FC component manufacturing and EoL is higher (i.e., 4% and 8%, respectively) due to both the larger system size (i.e., 400 kW instead of 200 kW) and FC replacement during the truck's lifetime. This involves the need for higher amounts of materials to produce the fuel cell and more impactful disposal.

3.3. LCA Results other than Climate Change at the Cradle-to-Gate Boundary

Figure 4 shows the comprehensive LCA results related to the fuel cell system for the cradle-to-gate boundary. All the scenarios considered in this study are shown. For scenario A, ozone depletion is 9.9E-05 kg CFC11 eq/kW. The main contribution is provided by BOP (51%), membrane (32%) and GDL (15%). For scenario B, ozone depletion is 8.7E-05 kg CFC11 eq/kW. The main contribution is provided by BOP (58%), membrane (22%), and GDL (19%). For scenario C, ozone depletion is 8.9E-05 kg CFC11 eq/kW. The main contribution is provided by BOP (57%), membrane (19%), and GDL (23%). For the optimistic scenario, ozone depletion is 6.0E-05 kg CFC11 eq/kW. The main contribution is provided by BOP (42%), membrane (28%), and GDL (27%). For the pessimistic scenario, the ozone depletion is 1.0E4 kg CFC11 eq/kW. The main contribution is provided by BOP (48%), membrane (30%), and GDL (19%). For BOP, the impact in ozone depletion is driven by the water management system, and more specifically by the TFE. In fact, the production of TFE can affect ozone depletion, involving the release of PFCs, which are potent ozone-depleting substances. Also, for the membrane and GDL, the cause can be attributed to TFE.

For scenario A, ionizing radiation is 3.03 kBq U-235 eq/kW. In this case, the main contribution is provided by BOP (27%), and catalyst (54%). For scenario B, ionizing radiation is 2.42 kBq U-235 eq/kW. In this case, the main contribution is provided by BOP (34%), and catalyst (38%). For scenario C, ionizing radiation is 2.39 kBq U-235 eq/kW. In this case, the main contribution is provided by BOP (34%), and catalyst (38%). For the optimistic scenario, ionizing radiation is 2.5 kBq U-235 eq/kW. In this case, the main contribution is provided by BOP (34%), and catalyst (38%). For the pessimistic scenario, ionizing radiation is 2.5 kBq U-235 eq/kW. In this case, the main contribution is provided by BOP (26%), and catalyst (51%). For the BOP, carbon fiber reinforced plastic is the main source. Carbon fibers themselves are not radioactive, but the precursor materials used in their production processes may contain trace amounts of naturally occurring radioactive elements. These radioactive impurities can contribute to the overall ionizing radiation. The main contribution to ionizing radiation in the catalyst layer is linked to platinum. While platinum itself is not radioactive, it can be activated through neutron bombardment in certain industrial processes, making it a significant contributor to ionizing radiation in the catalyst layer of FCs.

For scenario A, photochemical ozone formation is 0.66 kg NMVOC/kW, and the main contribution is given by the platinum contained in the catalyst (92%). For scenario B and C, photochemical ozone formation is 0.38 kg NMVOC/kW and 0.37 kg NMVOC/kW, respectively, and the main contribution is given by the platinum contained in the catalyst (84% for both). For the optimistic scenario, the photochemical ozone formation is 0.35 kg NMVOC/kW, and the main contribution is given by the platinum contained in the catalyst (86%). For the pessimistic scenario, the photochemical ozone formation is 0.67 kg NMVOC/kW, and the main contribution is given by the platinum contained in the catalyst (91%). This is due to the blasting processing of platinum in South Africa (ZA). The extraction and processing of platinum ore often

FIGURE 4 Comprehensive LCA results for the cradle-to-gate boundary.

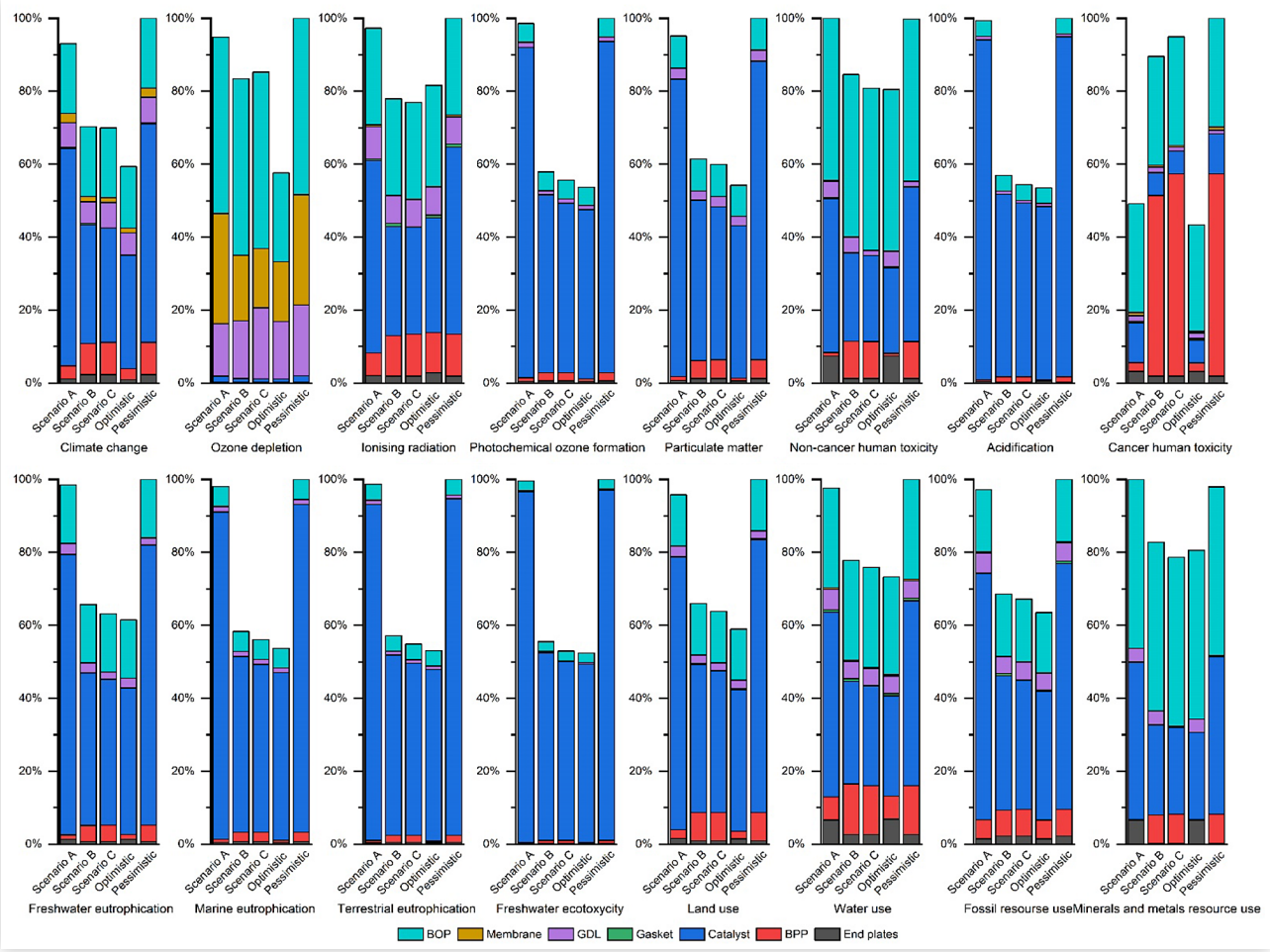

involves blasting techniques to access underground deposits. Blasting operations release particulate matter and aerosols into the atmosphere, which can contain platinum particles and compounds that contribute to photochemical ozone formation through complex atmospheric reactions.

For scenario A, B and C, particulate matter formation is 7.03E-06 disease inc/kW, 4.5E-06 disease inc/kW, and 4.4E-06 disease inc/kW respectively. This is due to the platinum contained in the catalyst (86%, 71%, and 70%, respectively). For the optimistic scenario, the particulate matter is 4.0E-06 disease inc/kW and 7.4E-06 disease inc/kW respectively, due to the platinum contained in the catalyst (77% and 82%, respectively). The reason is still attributable to platinum production technology (i.e., blasting).

For scenario A, non-cancer human toxicity is 1.9E-06 CTUh/kW. The main contributions are BOP and catalyst (44% and 42% respectively). For scenario B, non-cancer human toxicity is 1.7E-06 CTUh/kW. The main contributions are BOP and catalyst (53% and 29% respectively). For scenario C, non-cancer human toxicity is 1.6E-06 CTUh/kW. The main contributions are BOP and catalyst (55% and 29%). For the optimistic scenario, non-cancer human toxicity is 1.6E-06 CTUh/kW. The main contributions are BOP and catalyst (55% and 29% respectively). For the pessimistic scenario, non-cancer human toxicity is 2.0E-06 CTUh/kW. The main contributions are BOP and catalyst (45% and 42% respectively). In the case of BOP, the main contribution is linked to the copper contained in the cable conductors. In the case of catalyst, the blasting operation and the energy used for the metal production in South Africa drive this impact. In fact, the ZA electricity mix is based on 86% hard coal energy.

For scenario A, cancer human toxicity is 7.4E-08 CTUh/kW. The impact is driven by BOP and catalyst (61% and 22%). For scenario B, cancer human toxicity is 1.4E-07 CTUh/kW. The impact is driven by BOP and BPP (33% and 55%). For scenario C, cancer human toxicity, is 1.4E-07 CTUh/kW. The impact is driven by BOP and BPP (31% and 58%). For the optimistic scenario, cancer human toxicity is 6.5E-08 CTUh/kW. The impact is driven by BOP and catalyst (67% and 14%). For the pessimistic scenario, cancer human toxicity is 1.5E-07 CTUh/kW. The impact is driven by BOP and BPP (30% and 55%). For the BOP, the contribution derives from the production of chromium steel contained in the water and fuel management systems, and from copper production contained in the cable conductors. For the catalyst, platinum production

is the main driver to this impact while for the BPP chromium steel production is the main driver.

For scenario A, B and C, acidification is 2.3 mol H+ eq/kW, 1.3 mol H+ eq/kW, and 1.25 mol H+ eq/kW, respectively. Most of the contribution comes from the platinum in the catalyst (94%, 88%, and 88%, respectively). For the optimistic scenario, acidification is 1.23 mol H+ eq/kW while, for the pessimistic scenario, it is 2.3 mol H+ eq/kW. Most of the contribution comes from the platinum in the catalyst (89%, and 93%, respectively). The extraction and processing of platinum ore, particularly in regions like South Africa where platinum mining is prevalent, can lead to the release of sulfur dioxide (SO_2) and nitrogen oxides (NO_x) into the atmosphere. These emissions occur primarily as byproducts of the combustion of fossil fuels used in mining equipment, transportation, and energy-intensive processing techniques.

For scenario A, B and C, freshwater eutrophication is 0.05vkg P eq/kW, 0.03vkg P eq/kW and 0.03vkg P eq/kW, respectively. Platinum production of catalyst is the primary input (78%, 64% and 63%, respectively). For the optimistic scenario, freshwater eutrophication is 0.03 vkg P eq/kW. Platinum production of catalyst is the primary input (65%). For the pessimistic scenario, freshwater eutrophication is 0.049 vkg P eq/kW. Platinum production of catalyst is the primary input (77%). Eutrophication can be attributed to sulfidic tailings. The sulfidic tailings can indeed be generated from platinum mining processes, particularly when platinum ores contain sulfide minerals as part of their composition. Sulfidic tailings release sulfates and heavy metals into water bodies, promoting algal blooms and disrupting aquatic ecosystems.

For scenario A, B and C, marine eutrophication is 0.19 kg N eq/kW, 0.11 kg N eq/kW and 0.1 kg N eq/kW, respectively. In these case catalyst plays an important role because of platinum for 91%, 83% and 82%, respectively. For the optimistic scenario, the marine eutrophication is 0.1 kg N eq/kW. For the pessimistic scenario, the marine eutrophication is 0.18 kg N eq/kW. Most of the contribution comes from the platinum in the catalyst (86% and 90%, respectively) The blasting operation and the energy used for the platinum production in South Africa strongly affect this impact category.

For scenario A, B, and C, terrestrial eutrophication is 2.6 mol N eq/kW, 1.54 mol N eq/kW, and 1.47 mol N eq/kW, respectively. The platinum in the catalyst represents the main driver of this impact (93 %, 87%, and 86% respectively). For the optimistic scenario, terrestrial eutrophication is 1,43 mol N eq/kW. The platinum in the catalyst represents the main driver of this impact (89%). For the pessimistic scenario, terrestrial eutrophication is 2.69 mol N eq/kW. The platinum in the catalyst represents the main driver of this impact (92%).

For scenario A, B, and C, the freshwater ecotoxicity is 26614 CTUeq/kW, 14841 CTUeq/, 14147 CTUeq/kW, respectively, and the main impact contribution comes from platinum in the catalyst (97%, 93%, and 93%, respectively). For the optimistic scenario, the freshwater ecotoxicity is 14000 CTUeq/kW and the main impact contribution comes from platinum (94%). For the pessimistic scenario, the freshwater ecotoxicity is 26734 CTUeq/kW and the main impact contribution comes from platinum (96%).

For scenario A, B and C, land use is 343.5 Pt/kW, 236.5 Pt/kW and 228.5 Pt/kW, respectively. Platinum in the catalyst represents the main contribution of this impact category. Platinum contribution is equal to 78%, 61% and 61%, respectively. For the optimistic scenario, land use is 211.4 Pt/kW. For the pessimistic scenario, land use is 358.5 Pt/kW. The platinum in the catalyst represents the main driver of this impact (66 % and 75%, respectively). The main contribution is linked to platinum because of the extraction and processing of platinum ore, which can lead to habitat destruction, ecosystem disruption, and land degradation.

For scenario A, the water use is 11.98 m^3 depriv. The main contribution comes from catalyst and BOP (52% and 28%). For scenario B, the water use is 9.5 m^3 depriv. The main contribution comes from catalyst and BOP (36% and 35%). For scenario C, the water use is 9.3 m^3 depriv. The main contribution comes from catalyst and BOP (36% and 36%). For the optimistic scenario, the water use is 8.9 m^3 depriv. The main contribution comes from catalyst and BOP (37% and 37%). For the pessimistic scenario, the water use is 12.2 m^3 depriv. The main contribution comes from catalyst and BOP (51% and 27%). The platinum contained in the catalyst can have a significant impact on the water use impact category primarily due to the water-intensive processes involved in platinum mining, extraction, and processing. For BOP the main contribution comes from copper contained in cable conductors and from carbon fiber reinforced plastic contained in the belly pan component. Copper is typically extracted from copper ore through mining operations, which require significant amounts of water for ore processing, mineral separation, and waste management. Also, carbon fiber reinforced plastic production involves several water-intensive steps.

For scenario A, the fossil resource use is 657 MJ/kW. The main contribution comes from catalyst and BOP (69% and 18%). For scenario B, the fossil resource use is 463 MJ/kW. The main contribution comes from catalyst and BOP (54% and 25%). For scenario C, the fossil resource use is 454 MJ/kW. The main contribution comes from catalyst and BOP (53% and 25%). For the optimistic scenario, the fossil resource use is 429 MJ/kW. The main contribution comes from catalyst and BOP (56% and 26%). For the pessimistic scenario, the fossil resource use is 675 MJ/kW. The main contribution comes from catalyst and BOP (67% and 17%). The platinum contained in the catalyst strongly affects this impact category while, for BOP, the main contribution comes from copper contained in cable conductors and from carbon fiber reinforced plastic contained in the belly pan component.

For scenario A, mineral and metal resource use accounts for 3.9E-3 kg Sb eq/kW. The main contribution comes from catalyst and BOP (43% and 46%). For scenario B, mineral and metal resource use accounts for 3.2E-3 kg Sb eq/kW. The main contribution comes from catalyst and BOP (30% and 56%). For scenario C, mineral and metal resource use accounts for 3.1E3- kg Sb eq/kW. The main

contribution comes from catalyst and BOP (30% and 59%). For the optimistic scenario, mineral and metal resource use accounts for 3.1E-3 kg Sb eq/kW. The main contribution comes from catalyst and BOP (30% and 57%). For the pessimistic scenario mineral and metal resource use accounts for 3.8E-3 kg Sb eq/kW. The main contribution comes from catalyst and BOP (44% and 47%). For the catalyst, platinum production is the main source, while, for BOP, the main contribution comes from copper contained in cable conductors.

3.4. LCA Results other than Climate Change at the Cradle-to-Grave Boundary

Figure 5 shows the comprehensive LCA results for the cradle-to-grave boundary in a radar diagram. All the scenarios considered in this study are shown. The impacts are normalized to the highest score in each category. The use phase strongly affects all the impact categories, in fact, it ranges between 44-99%, depending on the impact category considered.

Scenario C (characterized by AE with fossil-based electricity as the hydrogen production route) resulted as the worst scenario in the categories of climate change, terrestrial eutrophication, land use, fossil resource use, ionizing radiation, photochemical ozone formation, acidification, and freshwater eutrophication. The reason is the adoption of the EU electricity mix, which is still heavily based on fossil fuels. The pessimistic scenario (characterized by SMR as the hydrogen production route) is the worst scenario in the categories of mineral and metal resource use, ozone depletion, particulate matter formation, non-cancer human toxicity, cancer human toxicity, marine eutrophication, freshwater ecotoxicity. The optimistic scenario (characterized by the AE with wind-based electricity mix) represents the best scenario in all categories, except for mineral and metal resource use and cancer human toxicity. In fact, for these two categories, scenario B (characterized by SMR with CCS as the hydrogen production route) represents the best scenario.

FIGURE 5 Comprehensive LCA results for the cradle-to-grave boundary

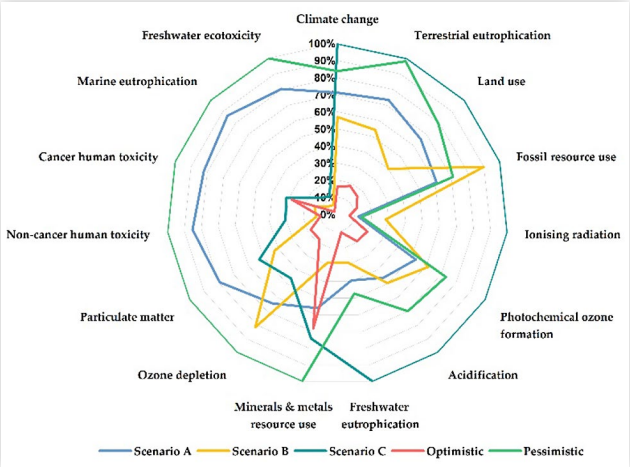

4. Conclusions

In recent years, climate change has become an increasingly topical and significant issue. Europe has set the important goal of achieving zero GHG emissions by 2050. However, to reach this target, several changes are needed. Many studies focused on the transport sector, which represents one of the most impactful in terms of GHG emissions. Nevertheless, there are many gaps in what concerns HDVs. The purpose of the present study is to investigate the environmental impacts of a 200-kW PEMFC over its entire life cycle, intended to be used on a zero-emission heavy-duty truck weighing 40 tons and with a driving range of 750 km. In addition, because the vehicle is still under design and it is going to be developed as a prototype in the next months, a scenario analysis was carried out on the following key parameters of the FC system: material composition, hydrogen production route, fuel consumption, production site, maximum power, and potential replacement during the vehicle lifetime. In fact, for the material composition, after conducting an extensive literature analysis on LCA research regarding PEMFCs, it has been found that there is no standard material composition. A fuel cell consists of several components (i.e., membrane, GDL, catalyst, BPP, EP, gasket, BOP) highly variable in terms of material breakdown. Another paramount contribution to the life cycle emissions of a FC system is given by the use phase. Hence, the present study investigated the effect of both diverse hydrogen production routes and fuel consumption. Four hydrogen production routes have been compared, namely SMR, SMR with CCS, AE with fossil-based electricity mix and AE with wind-based electricity mix. Two fuel consumptions have been compared, namely the specific fuel consumption of the truck under study and a more pessimistic value to consider an efficiency reduction linked to the FC degradation over time. Moreover, three different production sites have been compared because the country electricity mix is a paramount assumption in an LCA study and significantly impacts the outcomes. Lastly, the effects of a different FC system sizing and its potential replacement during the vehicle's lifetime have been explored. As a summary, five scenarios have been set up to investigate how the environmental impacts vary depending on the combination of the previous assumptions.

The analysis on climate change (i.e., GWP or GHG emissions) at the cradle-to-gate boundary identified the catalyst as the most impactful component due to the presence of platinum. This is because platinum production, which includes mining, processing, and refining, requires substantial energy consumption and results in harmful GHG emissions. In fact, reducing the platinum loading by 50% in scenarios B, C, and optimistic leads to

a significant reduction in the GWP of the catalyst itself and of the overall FC system. Furthermore, the BOP makes the second highest impact on climate change since it accounts for 60 v/v% of the FC system. The impact on climate change of BOP is due to the production of the carbon fiber reinforced plastic contained in the belly pan component and the copper contained in the cable conductor. Among all the scenarios considered in the present study, in the optimistic scenario, the GWP is the lowest, resulting in 30.5 kg CO2eq/kW. In this scenario, it has been assumed that the production takes place in Europe, which has made significant strides in transitioning to cleaner energy sources, including renewables and natural gas, reducing the overall GWP of the FC system. In conclusion, at the cradle-to-gate boundary, the GWP is closely influenced by three factors. First, the production site of the raw materials and FC components. Second, the platinum content, which is the reason why the catalyst represents the most impactful component. Further research is needed to evaluate the performance of the FC system in the case of reduced platinum content or in the case of substitution with secondary platinum. Lastly, the carbon fiber reinforced plastic contained in the belly pan component and copper contained in cable conductors, which is the reason why the BOP represents the second most impactful component. These results were consistent with the values reported in the literature.

The same analysis at the cradle-to-grave boundary revealed that the impacts related to the acquisition and preprocessing of raw materials and production of FC components are almost negligible when climate change is considered. In fact, the use phase contributes to the overall impact of the FC system by approximately 44-99%, varying depending on the scenario. The SMR and AE with fossil-based electricity mix, resulted in the most impactful hydrogen production routes.

When considering other impact categories, certain equivalences can be identified. At the cradle-to-gate boundary, the catalyst represents the most impactful component for almost all impact categories, except for ozone depletion and cancer human toxicity. In fact, BOP is the major contributor in the ozone depletion category due to TFE contained in the water management system. Also, the membrane and GDL are the second and third contributors in the ozone depletion category due to the presence of TFE. For cancer human toxicity, the BPP plays an important role due to the chromium steel. At the cradle to grave boundary, scenario C and pessimistic (with SMR and AE with fossil-based electricity mix as hydrogen production routes, respectively) resulted as the worst cases in many of the impact categories. Instead, the optimistic scenario adopting AE with wind-based electricity mix resulted as the most promising scenario.

Because platinum resulted to be one of the main driver to the impacts, further analysis on its potential recycling are needed. Lastly, enlarging the scope to the entire vehicle may change the results obtained in this study, giving a more comprehensive and broad view of the impacts of FC heavy duty trucks.

References

1. European Commission, "Reducing CO_2 Emissions from Heavy-Duty Vehicles - European Commission," 2024, accessed March 26, 2024, https://climate.ec.europa.eu/eu-action/transport/road-transport-reducing-co2-emissions-vehicles/reducing-co2-emissions-heavy-duty-vehicles_en.
2. European Environment Agency, "Greenhouse Gas Emissions from Transport in Europe 2023," accessed March 26, 2024, https://www.eea.europa.eu/en/analysis/indicators/greenhouse-gas-emissions-from-transport.
3. European Council, "Heavy-Duty Vehicles: Council and Parliament Reach a Deal to Lower CO_2 Emissions from Trucks, Buses and Trailers," 2024, accessed March 26, 2024, https://www.consilium.europa.eu/en/press/press-releases/2024/01/18/heavy-duty-vehicles-council-and-parliament-reach-a-deal-to-lower-co2-emissions-from-trucks-buses-and-trailers/.
4. Council of the European Union, "Proposal for a Regulation of the European Parliament and of the Council Amending Regulation (EU) 2019/1242 as Regards Strengthening the CO_2 Emission Performance Standards for New Heavyduty Vehicles and Integrating Reporting Obligations, and Repealing Regulation (EU) 2018/956," 2024.
5. Radley-Gardner, O., Beale, H., and Zimmermann, R. (Eds), *Regulation (EU) 2024/1610 of the European Parliament and of the Council*, 2nd ed. (Hart Publishing Ltd, 2024), https://doi.org/10.5040/9781782258674
6. Arrigoni, A., Arosio, V., Basso Peressut, A., Latorrata, S. et al., "Greenhouse Gas Implications of Extending the Service Life of PEM Fuel Cells for Automotive Applications: A Life Cycle Assessment," *Clean Technol* 4 (2022): 132-148, https://doi.org/10.3390/cleantechnol4010009.
7. Chen, Y., Hu, X., and Liu, J., "Life Cycle Assessment of Fuel Cell Vehicles Considering the Detailed Vehicle Components: Comparison and Scenario Analysis in China Based on Different Hydrogen Production Schemes," *Energies* 12 (2019): 3031, https://doi.org/10.3390/en12153031.
8. Bekel, K. and Pauliuk, S., "Prospective Cost and Environmental Impact Assessment of Battery and Fuel Cell Electric Vehicles in Germany," *Int J Life Cycle Assess* 24 (2019): 2220-2237, https://doi.org/10.1007/s11367-019-01640-8.
9. Drawer, C., Rödl, A., and Kaltschmitt, M., "Life Cycle Assessment of Construction and Driving Operation of a Hydrogen-Powered Truck Built from a Used Diesel Truck," *Transportation Research Interdisciplinary Perspectives* 24 (2024): 101020, https://doi.org/10.1016/j.trip.2024.101020.
10. Evangelisti, S., Tagliaferri, C., Brett, D.J.L., and Lettieri, P., "Life Cycle Assessment of a Polymer Electrolyte Membrane Fuel Cell System for Passenger Vehicles," *Journal of Cleaner Production* 142 (2017): 4339-4355, https://doi.org/10.1016/j.jclepro.2016.11.159.
11. Miotti, M., Hofer, J., and Bauer, C., "Integrated Environmental and Economic Assessment of Current

and Future Fuel Cell Vehicles," *Int J Life Cycle Assess* 22 (2017): 94-110, https://doi.org/10.1007/s11367-015-0986-4.

12. Simons, S. and Azimov, U., "Comparative Life Cycle Assessment of Propulsion Systems for Heavy-Duty Transport Applications," *Energies* 14 (2021): 3079, https://doi.org/10.3390/en14113079.
13. Velandia Vargas, J.E. and Seabra, J.E.A., "Fuel-Cell Technologies for Private Vehicles in Brazil: Environmental Mirage or Prospective Romance? A Comparative Life Cycle Assessment of PEMFC and SOFC Light-Duty Vehicles," *Science of The Total Environment* 798 (2021): 149265, https://doi.org/10.1016/j.scitotenv.2021.149265.
14. Simons, A. and Bauer, C., "A Life-Cycle Perspective on Automotive Fuel Cells," *Applied Energy* 157 (2015): 884-896, https://doi.org/10.1016/j.apenergy.2015.02.049.
15. Duclos, L., Lupsea, M., Mandil, G., Svecova, L. et al., "Environmental Assessment of Proton Exchange Membrane Fuel Cell Platinum Catalyst Recycling," *Journal of Cleaner Production* 142 (2017): 2618-2628, https://doi.org/10.1016/j.jclepro.2016.10.197.
16. British Standards Institute Staff, "Environmental Management. Life Cycle Assessment. Principles and Framework. Place of Publication Not Identified: Bsi," ISO 14040, 2006.
17. British Standards Institute Staff, "Environmental Management. Life Cycle Assessment. Requirements and Guidelines. Withdrawn," ISO 14044, 2018.
18. FC_Guidance_Document.pdf n.d.
19. Drawer, C., Rödl, A., and Kaltschmitt, M., "Life Cycle Assessment of Construction and Driving Operation of a Hydrogen-Powered Truck Built from a Used Diesel Truck," *Transportation Research Interdisciplinary Perspectives* 24 (2024): 101020, https://doi.org/10.1016/j.trip.2024.101020.
20. "PRé Sustainability B.V. SimaPro," 2024.
21. Ecoinvent, "Ecoinvent v.3.8 at the Point of Substitution (APOS) Database," 2021.
22. Zampori, L. and Pant, R., "Suggestions for updating the Product Environmental Footprint (PEF) Method," 2019.
23. British Standards Institution, "Environmental Management - Life Cycle Assessment - Principles and Framework," BS EN ISO 14040:2006, 2006.
24. Duclos, L., Lupsea, M., Mandil, G., Svecova, L. et al., "Environmental Assessment of Proton Exchange Membrane Fuel Cell Platinum Catalyst Recycling," *Journal of Cleaner Production* 142 (2017): 2618-2628, https://doi.org/10.1016/j.jclepro.2016.10.197.
25. Hickner, M.A., Ghassemi, H., Kim, Y.S., Einsla, B.R. et al., "Alternative Polymer Systems for Proton Exchange Membranes (PEMs)," *Chem Rev* 104 (2004): 4587-4612, https://doi.org/10.1021/cr020711a.
26. Wang, Y., Ruiz Diaz, D.F., Chen, K.S., Wang, Z. et al., "Materials, Technological Status, and Fundamentals of PEM Fuel Cells – A Review," *Materials Today* 32 (2020): 178-203, https://doi.org/10.1016/j.mattod.2019.06.005.
27. Brett, D.J.L. and Brandon, N.P., "Review of Materials and Characterization Methods for Polymer Electrolyte Fuel Cell Flow-Field Plates," *Journal of Fuel Cell Science and Technology* 4 (2007): 29-44, https://doi.org/10.1115/1.2393303.
28. Millichamp, J., Mason, T.J., Neville, T.P., Rajalakshmi, N. et al., "Mechanisms and Effects of Mechanical Compression and Dimensional Change in Polymer Electrolyte Fuel Cells – A Review," *Journal of Power Sources* 284 (2015): 305-320, https://doi.org/10.1016/j.jpowsour.2015.02.111.
29. Carlson, E.J., Kopf, P., Sinha, J., Sriramulu, S. et al., "Cost Analysis of PEM Fuel Cell Systems for Transportation: September 30, 2005," 2005, https://doi.org/10.2172/862302.
30. AIT Austrian Institute of Technology GMBH, "Hydrogen Consumption Estimation," 2024.
31. Ahmadi, P. and Khoshnevisan, A., "Dynamic Simulation and Lifecycle Assessment of Hydrogen Fuel Cell Electric Vehicles Considering Various Hydrogen Production Methods," *International Journal of Hydrogen Energy* 47 (2022): 26758-26769, https://doi.org/10.1016/j.ijhydene.2022.06.215.
32. Benitez, A., Wulf, C., De Palmenaer, A., Lengersdorf, M. et al., "Ecological Assessment of Fuel Cell Electric Vehicles with Special Focus on Type IV Carbon Fiber Hydrogen Tank," *Journal of Cleaner Production* 278 (2021): 123277, https://doi.org/10.1016/j.jclepro.2020.123277.
33. Usai, L., Hung, C.R., Vásquez, F., Windsheimer, M. et al., "Life Cycle Assessment of Fuel Cell Systems for Light Duty Vehicles, Current State-of-the-Art and Future Impacts," *Journal of Cleaner Production* 280 (2021): 125086, https://doi.org/10.1016/j.jclepro.2020.125086.

Contact Information

Corresponding authors:
Antonella Accardo
Politecnico di Torino. Dipartimento Energia "G. Ferraris", CARS@Polito. Corso Francesco Ferrucci, 112, 10129 Torino, Italy
antonella.accardo@polito.it

Gaia Gentilucci
Politecnico di Torino. Dipartimento Energia "G. Ferraris" CARS@Polito. Corso Francesco Ferrucci, 112, 10129 Torino, Italy
gaia.gentilucci@polito.it

Acknowledgments

This research has been funded by the European Union's Horizon Europe research and innovation programme under GA No 101096028. This work is part of the research activities of the interdepartmental Center for Automotive Research and Sustainable mobility (CARS) of Politecnico di Torino.

Funded by the European Union. Views and opinions expressed are however those of the author(s) only and do not necessarily reflect those of the European Union or the European Climate, Infrastructure and Environment Executive Agency (CINEA). Neither the European Union nor CINEA can be held responsible for them.

ISSN 0148-7191